Proceedings of the 2006 IEEE International Conference on Robotics and Automation
Orlando, Florida - May 2006

A Quantitative Test for the Robustness of Graspless Manipulation

Yusuke MAEDA
Dept. of Systems Design, Div. of Systems Research,
Fac. of Engineering,
Yokohama National University
79-5 Tokiwadai, Hodogaya-ku, Yokohama
240-8501 JAPAN
Email: maeda@ynu.ac.jp

Satoshi MAKITA
Maeda Lab, Dept. of Mechanical Engineering,
Div. of Systems Integration, Graduate School of Engineering,
Yokohama National University
79-5 Tokiwadai, Hodogaya-ku, Yokohama
240-8501 JAPAN
Email: makita@iir.me.ynu.ac.jp

Abstract— **In this paper, the robustness of graspless manipulation (or nonprehensile manipulation) is investigated. We derive some new constraints for static frictional forces in graspless manipulation, which gives us more accurate evaluation of the robustness of graspless manipulation than previous studies. We also present a procedure to calculate a measure of the robustness based on linear programming. Numerical examples are shown to prove that our new method works well even when previous methods make an inappropriate evaluation.**

I. Introduction

Graspless manipulation [1] (or nonprehensile manipulation [2]) is a method to manipulate objects without grasping. In this paper, we deal with graspless manipulation where the manipulated object is supported not only by robot fingers but also by the environment; it includes pushing, sliding and tumbling (Fig. 1). Graspless manipulation brings the following advantages to robots:

- Manipulation without supporting all the weight of the object.
- Manipulation with simple mechanisms.
- Manipulation when grasping is impossible.

Thus, graspless manipulation is important as a complement of pick-and-place for the dexterity of robots.

Graspless manipulation is obviously inferior to pick-and-place with regard to the robustness against external disturbances. Therefore it is important to develop a robustness measure for planning and execution of graspless manipulation. Consider graspless manipulation as shown in Fig. 2. A stationary object on a frictional plane (Fig. 2, upper left) can be regarded as "robust"; it can resist external disturbances to some extent with the help of friction and gravity. The same stationary object in one-point contact with a robot finger (Fig. 2, upper right) is also robust against external disturbances. However, the same object in motion pushed by the same finger (Fig. 2, lower left) is not robust; the path of the object would be perturbed easily. On the other hand, the same object pushed by two position-controlled robot fingers (Fig. 2, lower right) is robust because the object can keep going on a straight path even against external disturbances to some degree; that corresponds to a "stable push" [3]. We need a quantitative test that can evaluate the robustness in such situations appropriately.

Although there are so many quality measures for grasps [4]–[6], few of their results can be applied to graspless manipulation straightforwardly. Mason and Lynch presented the notions of "quasi-static closure" and "dynamic closure" [7], but they were not mathematically formulated. Trinkle et al. formulated "first-order stability" in detail for whole-arm manipulation [8]. Although the first-order stability would be also valid for graspless manipulation, they presented no quality measure for it. Kijimoto et al. proposed a performance index for quasi-static graspless manipulation [9]. However, the physical meaning of the index is unclear, especially in cases where sliding contacts or surface/line contacts exist.

Maeda and Arai [10] presented a robustness measure for graspless manipulation that evaluates how much the manipulated object can resist external disturbances without changing its motion. Although the measure can deal with the situations as shown in Fig. 2, it overestimates the robustness of graspless

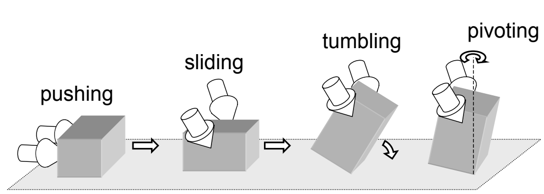

Fig. 1. Graspless Manipulation

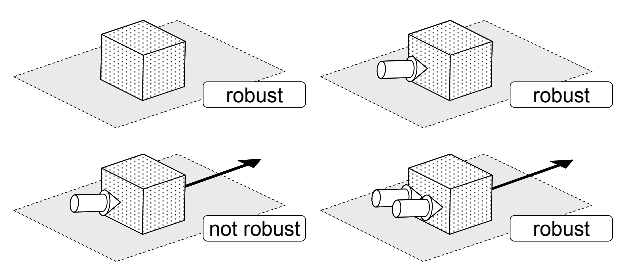

Fig. 2. Robustness of Graspless Manipulation

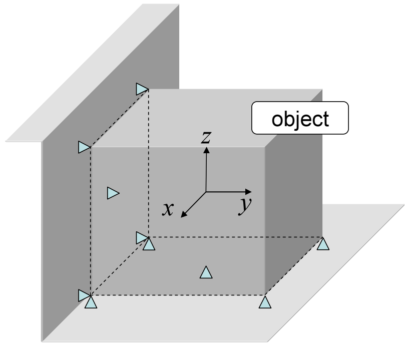

Fig. 3. An Object on a Corner

manipulation in some cases. For example, let us consider a stationary cube on a right-angled corner as shown in Fig. 3. In this case, the value of the measure in [10] diverges to infinity for the friction coefficient larger than 1.0 (see examples in Section V); that is, we cannot move this object even with infinite external forces—of course, this result is unreasonable.

In this paper, we propose a new quantitative test for the robustness of graspless manipulation. We adopt the definition of the measure in [10] but modify the calculation procedure of the measure by considering some new constraints, which were originally derived by Omata and Nagata [11] [12] for power grasps, on static frictional forces. The new calculation method leads to improved accuracy of robustness evaluation for graspless manipulation.

II. Assumptions

In this paper, for graspless manipulation by multiple robot fingers (as shown in Fig. 4), we make the following assumptions:

1) The manipulated object, robot fingertips, and environment are rigid.
2) The object is stationary or in quasi-static manipulation.
3) Coulomb friction exists between the object and the environment (or the robot fingertips).
4) All the contacts can be approximated by finite-point contacts.
5) Each friction cone can be approximated by a polyhedral convex cone [13].
6) Contacts with robot fingers are not defective [14] [15].
7) Each robot finger is either in position-control mode or in force-control mode.
   a) Each robot finger in position-control mode can passively apply arbitrary force within its friction cone.
   b) Each robot finger in force-control mode is in hybrid position/force control [16]; the finger can actively apply a commanded normal force and passively apply arbitrary tangential force within its friction cone.
8) The servo stiffness of the robot finger in position-control mode is infinite.

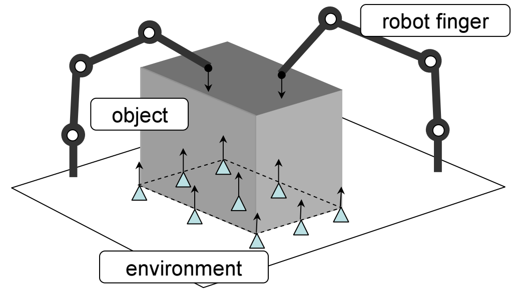

Fig. 4. Object in Graspless Manipulation

III. Mechanical Model

A. Contact Forces

Let $\boldsymbol{p}_1, \ldots, \boldsymbol{p}_M \in \Re^3$ be the positions of the contact points between the object and the environment (or the robot fingertips). All the contact points can be classified into two groups: contacts in actual sliding and those not. Thus, we define:

$$d_i := \begin{cases} 1 & \text{when the } i\text{-th contact point is in actual sliding,} \\ 0 & \text{otherwise.} \end{cases} \tag{1}$$

Then contact force at the i-th contact point, $\boldsymbol{f}_i (\in \Re^3)$, can be expressed as:

$$\boldsymbol{f}_i = \boldsymbol{C}_i \boldsymbol{k}_i, \tag{2}$$

where

$$\boldsymbol{C}_i := \begin{cases} [\boldsymbol{c}_{i1} \ \ldots \ \boldsymbol{c}_{is}] \in \Re^{3\times s_i}, \ s_i = s & \text{when } d_i = 0, \\ [\boldsymbol{c}'_i] \in \Re^{3\times s_i}, \ s_i = 1 & \text{when } d_i = 1; \end{cases} \tag{3}$$

$\boldsymbol{c}_{i1}, \ldots, \boldsymbol{c}_{is} \in \Re^3$ are the unit edge vectors of a polyhedral convex cone that approximates the friction cone at the i-th contact point; $\boldsymbol{c}'_i \in \Re^3$ is a unit edge vector of the friction cone at the i-th contact point opposite to its sliding direction; $\boldsymbol{k}_i := [k_{i1}, \ldots, k_{is_i}]^T \in \Re^{s_i}$ and $\boldsymbol{k}_i \geq \boldsymbol{0}$.

For the contacts with robot fingers in force-control mode, the following additional constraint must be satisfied:

$$\boldsymbol{n}_i^T \boldsymbol{f}_i = f_{\mathrm{com}\, i}, \tag{4}$$

where $\boldsymbol{n}_i \in \Re^3$ is the inward-pointing unit normal vector at the i-th contact and $f_{\mathrm{com}\, i} (\geq 0)$ is the magnitude of the commanded normal force of the corresponding robot finger.

Then we define the following matrices:

$$\boldsymbol{W} := \begin{bmatrix} \boldsymbol{I}_3 & \ldots & \boldsymbol{I}_3 \\ \boldsymbol{p}_1 \times \boldsymbol{I}_3 & \ldots & \boldsymbol{p}_M \times \boldsymbol{I}_3 \end{bmatrix} \in \Re^{6\times 3M} \tag{5}$$

$$\boldsymbol{C} := \mathrm{diag}(\boldsymbol{C}_1, \ldots, \boldsymbol{C}_M) \in \Re^{3M\times \tilde{s}} \tag{6}$$

$$\boldsymbol{N} := \mathrm{diag}(\boldsymbol{n}_1, \ldots, \boldsymbol{n}_M) \in \Re^{3M\times M} \tag{7}$$

$$\boldsymbol{T} := \mathrm{diag}(\boldsymbol{T}_1, \ldots, \boldsymbol{T}_M) \in \Re^{3M\times 2M} \tag{8}$$

$$\boldsymbol{T}_i := [\boldsymbol{t}_{i1} \ \boldsymbol{t}_{i2}] \in \Re^{3\times 2} \tag{9}$$

$$\boldsymbol{J} := \mathrm{diag}(\boldsymbol{J}_1, \ldots, \boldsymbol{J}_M) \in \Re^{3M\times L}, \tag{10}$$

where $\boldsymbol{I}_n$ is the $n \times n$ identity matrix; $\boldsymbol{p}_i \times \boldsymbol{I}_3 \in \Re^{3\times 3}$ is a skew-symmetric matrix defined such that $(\boldsymbol{p}_i \times \boldsymbol{I}_3)\boldsymbol{x} \equiv \boldsymbol{p}_i \times \boldsymbol{x}$;

$\tilde{s} := \sum_{i=1}^{M} s_i$; $\boldsymbol{t}_{i1}$, $\boldsymbol{t}_{i2} \in \Re^3$ are unit tangent vectors at the i-th contact defined such that $\boldsymbol{t}_{i1}^T \boldsymbol{t}_{i2} = 0$; $\boldsymbol{J}_i \in \Re^{3 \times L_i}$ is the Jacobian matrix between the position of the i-th contact point and joint variables of the corresponding robot finger; L_i is the number of joints of the robot finger (let $L_i = 0$ for the contacts with the environment); $L := \sum_{i=1}^{M} L_i$.

Now all the contact forces can be represented as follows:

$$\boldsymbol{f} = \boldsymbol{C}\boldsymbol{k}, \tag{11}$$

where $\boldsymbol{f} := \left[\boldsymbol{f}_1^T, \ldots, \boldsymbol{f}_M^T\right]^T \in \Re^{3M}$, $\boldsymbol{k} := \left[\boldsymbol{k}_1^T, \ldots, \boldsymbol{k}_M^T\right]^T \in \Re^{\tilde{s}}$ and $\boldsymbol{k} \geq \boldsymbol{0}$. All the tangential (=frictional) components of the contact forces are:

$$\boldsymbol{T}^T \boldsymbol{f} = \boldsymbol{T}^T \boldsymbol{C}\boldsymbol{k} \in \Re^{2M}. \tag{12}$$

The constraints on the contacts with robot fingers in force-control mode, (4), can be unified as follows:

$$\boldsymbol{A}(\boldsymbol{N}^T \boldsymbol{f} - \boldsymbol{f}_{\text{com}}) = \boldsymbol{A}(\boldsymbol{N}^T \boldsymbol{C}\boldsymbol{k} - \boldsymbol{f}_{\text{com}}) = \boldsymbol{0}, \tag{13}$$

where $\boldsymbol{A}$ is a selection matrix defined as:

$$\boldsymbol{A} := \operatorname{diag}(a_1, \ldots, a_M) \in \Re^{M \times M}, \tag{14}$$

$$a_i := \begin{cases} 1 & \text{when the } i\text{-th contact corresponds to a robot finger in force-control mode,} \\ 0 & \text{otherwise.} \end{cases} \tag{15}$$

and $\boldsymbol{f}_{\text{com}} := [f_{\text{com}\,1}, \ldots, f_{\text{com}\,M}]^T \in \Re^M$.

The resultant force/moment applied to the object by all the contact forces is given by:

$$\boldsymbol{W}\boldsymbol{f} = \boldsymbol{W}\boldsymbol{C}\boldsymbol{k} \in \Re^6. \tag{16}$$

Then the equilibrium equation of the object in quasi-static graspless manipulation can be expressed as follows:

$$\boldsymbol{Q}_{\text{dist}} + \boldsymbol{Q}_{\text{known}} + \boldsymbol{W}\boldsymbol{C}\boldsymbol{k} = \boldsymbol{0}, \tag{17}$$

where $\boldsymbol{Q}_{\text{dist}} \in \Re^6$ is an unknown external generalized force applied to the object by disturbances; $\boldsymbol{Q}_{\text{known}} \in \Re^6$ is a known external (generalized) force such as gravity.

B. Global Constraints on Possible Contact Forces

Static frictional forces on the contact points represented as (12) satisfy "local" constraints imposed by Coulomb's law. There exist, however, additional "global" constraints imposed by contact kinematics, which were derived by Omata and Nagata [11] [12] for power grasps. Here we show these additional constraints, which are slightly modified from the original formulation in [11] and [12] due to the application to graspless manipulation instead of power grasps.

Suppose a *virtual* infinitesimal motion of the object and the robots that causes *virtual* sliding at some contact points. Note that this virtual sliding is required only to derive the constraints on *static* frictional forces and must be distinguished from *actual* sliding, which corresponds to *kinetic* frictional forces.

TABLE I

RELATIONSHIP BETWEEN SLIDING AND FRICTION

Contacts in actual sliding ($d_i = 1$)	Contacts not in actual sliding ($d_i = 0$)	
	in virtual sliding ($b_i = 1$)	not in virtual sliding ($b_i = 0$)
kinetic friction	static friction	no friction

We define a selection matrix that selects contact points that will slide by the virtual motion as follows:

$$\boldsymbol{B} := \operatorname{diag}(b_1 \boldsymbol{I}_3, \ldots, b_M \boldsymbol{I}_3) \in \Re^{3M \times 3M}, \tag{18}$$

where

$$b_i := \begin{cases} 1 & \text{when the } i\text{-th contact point is in virtual sliding,} \\ 0 & \text{otherwise.} \end{cases} \tag{19}$$

From contact kinematics, the virtual motion corresponding to $\boldsymbol{B}$ must satisfy the following constraint:

$$\boldsymbol{B}\left(\begin{bmatrix}\boldsymbol{W}^T & \boldsymbol{J}\end{bmatrix}\begin{bmatrix}\boldsymbol{V} \\ -\dot{\boldsymbol{\theta}}\end{bmatrix} - \boldsymbol{T}\dot{\boldsymbol{Y}}\right) = \boldsymbol{0}, \tag{20}$$

where $\boldsymbol{V} = [\boldsymbol{v}^T \ \boldsymbol{\omega}^T]^T \in \Re^6$ is the (virtual) velocity/angular velocity of the object; $\dot{\boldsymbol{\theta}} = \left[\dot{\boldsymbol{\theta}}_1^T, \ldots, \dot{\boldsymbol{\theta}}_M^T\right]^T \in \Re^L$ and $\dot{\boldsymbol{\theta}}_i \in \Re^{L_i}$ is the (virtual) joint velocity vector of the robot corresponding to the i-th contact; $\dot{\boldsymbol{Y}} := \left[\dot{\boldsymbol{Y}}_1^T, \ldots, \dot{\boldsymbol{Y}}_M^T\right]^T \in \Re^{2M}$ and $\dot{\boldsymbol{Y}}_i = [\dot{Y}_{i1}, \dot{Y}_{i2}]^T \in \Re^2$ is the elements of the (virtual) sliding velocity vector at the i-th contact point (i.e., $\boldsymbol{T}_i \dot{\boldsymbol{Y}}_i$ is the sliding velocity vector).

Equation (20) constrains the possible $\dot{\boldsymbol{Y}}$; thus, the possible signs of the elements of $\dot{\boldsymbol{Y}}$ are restricted. The possible signs of the elements of frictional forces are also restricted, because static frictional forces can apply only in the directions that prevent virtual sliding.

Concretely, a combination of the signs of the elements of $\boldsymbol{T}^T \boldsymbol{C}\boldsymbol{k}$ is impossible if there exists no $\boldsymbol{B}$ that satisfies (20) for $\dot{\boldsymbol{Y}}$ whose elements have the same combination of their signs as $\boldsymbol{T}^T \boldsymbol{C}\boldsymbol{k}$. In other words, only $\boldsymbol{T}^T \boldsymbol{C}\boldsymbol{k}$ whose elements have the same combination of their signs as $\dot{\boldsymbol{Y}}$ that satisfies (20) is compatible with rigid-body motion.

Let us denote the set of static frictional forces that satisfy the above constraint on the signs of the elements by $\boldsymbol{\mathcal{F}}$, and then we have:

$$\boldsymbol{T}^T \boldsymbol{C}\boldsymbol{k} \in \boldsymbol{\mathcal{F}}. \tag{21}$$

Note again that we must distinguish between actual sliding and virtual sliding in this paper. Virtual sliding is just for deriving (21). The relationship between sliding and friction is summarized in Table I.

IV. ROBUSTNESS MEASURE

A. Formulation

The robustness measure for graspless manipulation defined in [10] evaluates how much the object can resist external disturbances without changing its motion. We also use this definition in this paper and then the value of the measure, z, can be written as follows:

$$z = \min_{\boldsymbol{Q}_{\text{dist}}} \max_{\boldsymbol{k}} \|\boldsymbol{Q}_{\text{known}} + \boldsymbol{W}\boldsymbol{C}\boldsymbol{k}\|_{\boldsymbol{R}} \tag{22}$$

$$\text{subject to} \begin{cases} \boldsymbol{T}^T\boldsymbol{C}\boldsymbol{k} \in \mathcal{F} \\ \boldsymbol{A}(\boldsymbol{N}^T\boldsymbol{C}\boldsymbol{k} - \boldsymbol{f}_n) = \boldsymbol{0} \\ \boldsymbol{Q}_{\text{dist}} + \boldsymbol{Q}_{\text{known}} + \boldsymbol{W}\boldsymbol{C}\boldsymbol{k} = \boldsymbol{0} \\ \|\boldsymbol{Q}_{\text{dist}}\|_{\boldsymbol{R}} = 1 \\ \boldsymbol{k} \geq \boldsymbol{0}. \end{cases}$$

$\boldsymbol{R} \in \Re^{6\times 6}$ is a positive definite matrix for scaling of force and moment, which is used to introduce the following norm for generalized forces, $\boldsymbol{Q} \in \Re^6$:

$$\|\boldsymbol{Q}\|_{\boldsymbol{R}} := \sqrt{\boldsymbol{Q}^T\boldsymbol{R}\boldsymbol{Q}} = \sqrt{(\boldsymbol{R}^{1/2}\boldsymbol{Q})^T(\boldsymbol{R}^{1/2}\boldsymbol{Q})}, \tag{23}$$

where $\boldsymbol{R}^{1/2} \in \Re^{6\times 6}$ is the Cholesky decomposition of $\boldsymbol{R}$. We can have a coordinate-invariant norm by using the following scaling matrix:

$$\boldsymbol{R} := \begin{bmatrix} \boldsymbol{I}_3 & \boldsymbol{O} \\ \boldsymbol{O} & M_o\boldsymbol{J}_o^{-1} \end{bmatrix} \in \Re^{6\times 6}, \tag{24}$$

where $M_o \in \Re$ is the mass of the object and $\boldsymbol{J}_o \in \Re^{3\times 3}$ is the inertia tensor of the object about the center of mass.

Note that the constraint on static frictional forces (21) is not considered in [10].

B. Calculation Procedure

It is not straightforward to solve the minimax optimization problem (22) directly because the constraint (21) is complicated. Thus, we divide (22) into subproblems so that (21) becomes linear.

To define the subproblems based on the signs of the elements of virtual sliding, we introduce the following matrix:

$$\boldsymbol{S} := \text{diag}(s_{11},\ s_{12},\ \ldots,\ s_{M1},\ s_{M2}) \in \Re^{2M\times 2M}, \tag{25}$$

where

$$s_{ij} := \begin{cases} +1 & \text{when } b_i = 1 \text{ and } \dot{Y}_{ij} > 0, \\ -1 & \text{when } b_i = 1 \text{ and } \dot{Y}_{ij} < 0, \\ 0 & \text{when } b_i = 0. \end{cases} \tag{26}$$

Then we have:

$$\dot{\boldsymbol{Y}} = \boldsymbol{S}\boldsymbol{q}, \tag{27}$$

where $\boldsymbol{q}(\in \Re^{2M}) > \boldsymbol{0}$.

The existence of $\boldsymbol{q}$ that satisfies (27) and (20) can be tested by solving the following linear programming problem:

$$\underset{\boldsymbol{q},\boldsymbol{V},\dot{\boldsymbol{\theta}}}{\text{maximize}}\ \boldsymbol{1}^T\boldsymbol{q}$$

$$\text{subject to} \begin{cases} \boldsymbol{B}\left(\begin{bmatrix}\boldsymbol{W}^T & \boldsymbol{J}\end{bmatrix}\begin{bmatrix}\boldsymbol{V} \\ -\dot{\boldsymbol{\theta}}\end{bmatrix} - \boldsymbol{T}\boldsymbol{S}\boldsymbol{q}\right) = \boldsymbol{0} \\ \boldsymbol{q} \geq \boldsymbol{1}, \end{cases} \tag{28}$$

where $\boldsymbol{1} = [1, \ldots, 1]^T \in \Re^{2M}$. When the objective function diverges to infinity, there exist $\boldsymbol{q}(> \boldsymbol{0})$ that satisfies (27) and (20). In that case, eq. (21) can be written in the following linear forms for a subcase specified by $\boldsymbol{S}$:

$$\boldsymbol{S}\boldsymbol{T}^T\boldsymbol{C}\boldsymbol{k} \leq \boldsymbol{0}, \tag{29}$$

$$\boldsymbol{T}^T(\boldsymbol{I}_{3M} - \boldsymbol{B} - \boldsymbol{D})\boldsymbol{C}\boldsymbol{k} = \boldsymbol{0}, \tag{30}$$

where $\boldsymbol{D}$ is a selection matrix defined as follows:

$$\boldsymbol{D} := \text{diag}(d_1\boldsymbol{I}_3, \ldots, d_M\boldsymbol{I}_3) \in \Re^{3M\times 3M}. \tag{31}$$

Inequality (29) means that static frictional forces can be applied only in the opposite directions of virtual sliding; eq. (30) means that the contact points that are neither in actual nor virtual sliding cannot apply frictional forces.

Thus, the problem (22) can be transformed into the following problem:

$$z = \min_{\boldsymbol{Q}_{\text{dist}}} \max_{\boldsymbol{k},\boldsymbol{B},\boldsymbol{S}} \|\boldsymbol{Q}_{\text{known}} + \boldsymbol{W}\boldsymbol{C}\boldsymbol{k}\|_{\boldsymbol{R}} \tag{32}$$

$$\text{subject to} \begin{cases} \boldsymbol{S}\boldsymbol{T}^T\boldsymbol{C}\boldsymbol{k} \leq \boldsymbol{0} \\ \boldsymbol{T}^T(\boldsymbol{I}_{3M} - \boldsymbol{B} - \boldsymbol{D})\boldsymbol{C}\boldsymbol{k} = \boldsymbol{0} \\ \boldsymbol{A}(\boldsymbol{N}^T\boldsymbol{C}\boldsymbol{k} - \boldsymbol{f}_n) = \boldsymbol{0} \\ \boldsymbol{Q}_{\text{dist}} + \boldsymbol{Q}_{\text{known}} + \boldsymbol{W}\boldsymbol{C}\boldsymbol{k} = \boldsymbol{0} \\ \|\boldsymbol{Q}_{\text{dist}}\|_{\boldsymbol{R}} = 1 \\ \boldsymbol{k} \geq \boldsymbol{0}. \end{cases}$$

Then the approximate value of z can be calculated by solving the following linear programming problems:

$$z = \min_i \max_j z_{ij} \tag{33}$$

$$z_{ij} = \max_{\zeta,\boldsymbol{k}} \zeta \tag{34}$$

$$\text{subject to} \begin{cases} \boldsymbol{S}_j\boldsymbol{T}^T\boldsymbol{C}\boldsymbol{k} \leq \boldsymbol{0} \\ \boldsymbol{T}^T(\boldsymbol{I}_{3M} - \boldsymbol{B}_j - \boldsymbol{D})\boldsymbol{C}\boldsymbol{k} = \boldsymbol{0} \\ \boldsymbol{A}(\boldsymbol{N}^T\boldsymbol{C}\boldsymbol{k} - \boldsymbol{f}_n) = \boldsymbol{0} \\ \zeta\boldsymbol{R}^{-1/2}\boldsymbol{l}_i + \boldsymbol{Q}_{\text{known}} + \boldsymbol{W}\boldsymbol{C}\boldsymbol{k} = \boldsymbol{0} \\ \boldsymbol{k} \geq \boldsymbol{0}, \end{cases}$$

where $\boldsymbol{l}_1, \ldots, \boldsymbol{l}_N \in \Re^6$ are position vectors of vertices of a hyperpolyhedron that approximates the six-dimensional unit hypersphere.

Now we can present a complete procedure for the calculation of the value of the robustness as follows:

Step 1. Enumerate all the combinations of virtual sliding/non-sliding contact points for contacts not in actual sliding (namely, enumerate selection matrices $\boldsymbol{B}$).

Step 2. Enumerate all the possible $\boldsymbol{S}$ for each $\boldsymbol{B}$ by solving the problem (28). There are 2^{2n} patterns for $\boldsymbol{S}$ at most when $\boldsymbol{B}$ selects n virtual sliding points.

Step 3. For each combination of $\boldsymbol{B}$ and $\boldsymbol{S}$, solve the problem (34).

Step 4. Obtain the robustness value from (33).

Considering the constraints on static frictional forces (21), the above procedure enables us to obtain more accurate estimation of the robustness of graspless manipulation than a previous study [10].

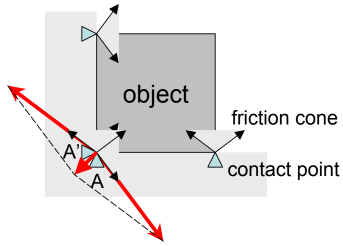

Fig. 5. Impossible Combination of Contact Forces (2D Schematic View)

If we implement the above procedure straightforwardly, we have to solve problem (34) $5^{\tilde{M}} \left(= \sum_{n=0}^{\tilde{M}} \binom{\tilde{M}}{n} 2^{2n}\right)$ times at most, where $\tilde{M} = M - \sum_{i=1}^{M} d_i$. However, some of them can be skipped by considering a property of problem (28). The problem (28) for a combination of $\boldsymbol{B}$ and $\boldsymbol{S}$ is a relaxation problem for other combinations. Therefore, if a combination of $\boldsymbol{B}$ and $\boldsymbol{S}$ is found impossible, we can omit some other combinations immediately.

V. Numerical Examples

We implemented the above procedure as a computer program, which uses GLPK (GNU Linear Programming Kit) to solve linear programming problems. Here we show some numerical examples calculated by this program. The computation times for the examples are measured on a Linux PC with Celeron–2.4GHz.

Let the manipulated object be a polyhedra, whose mass distribution is uniform; the gravitational acceleration is 9.8; each friction cone is represented as a polyhedral convex cone with 36 unit edge vectors ($s = 36$). We approximate surface contacts by point contacts at their vertices and centroids.

Here we adopt (24) as the scaling matrix for the norm of generalized forces. We use the following 76 points ($N = 76$) as the vertices of a hyperpolyhedron that approximates the six-dimensional unit hypersphere:

$$\begin{aligned}\{\boldsymbol{l}_i\} := \Big\{&[\pm 1,\ 0,\ 0,\ 0,\ 0,\ 0]^T,\ [0,\ \pm 1,\ 0,\ 0,\ 0,\ 0]^T,\\ &[0,\ 0,\ \pm 1,\ 0,\ 0,\ 0]^T,\ [0,\ 0,\ 0,\ \pm 1,\ 0,\ 0]^T,\\ &[0,\ 0,\ 0,\ 0,\ \pm 1,\ 0]^T,\ [0,\ 0,\ 0,\ 0,\ 0,\ \pm 1]^T,\\ &\frac{1}{\sqrt{6}}[\pm 1,\ \pm 1,\ \pm 1,\ \pm 1,\ \pm 1,\ \pm 1]^T\Big\}. \end{aligned} \quad (35)$$

A. Object on a Corner

Consider a stationary cube on a right-angled corner as shown in Fig. 3. In this case, there exist no robot fingers. The object reference frame is set as shown in the figure. The size of the object is $2 \times 2 \times 2$ and the mass of the object is 1 ($M_o = 1$). The surface contacts between the object and the environment are approximated by ten point contacts depicted in Fig. 3.

In this case, when the friction coefficient is larger than 1.0, the value of the measure in [10] becomes infinite; because some impossible combinations of contact forces illustrated in Fig. 5 are not excluded, the robustness is overestimated in [10].

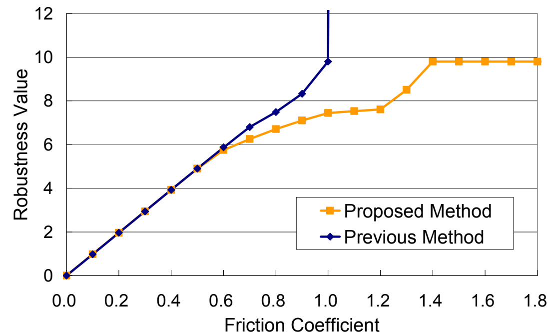

Fig. 6. Manipulation Robustness for an Object on a Corner

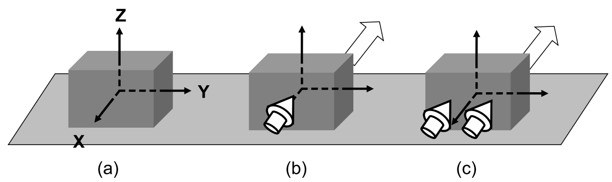

Fig. 7. Example: Pushing a Cuboid

On the other hand, such impossible combinations of contact forces are excluded in our new method because of the consideration of constraints on static frictional forces (21). See the relationship between the friction coefficient and the value of the manipulation robustness (Fig. 6). The robustness value in a previous method in [10] diverges to infinity when the friction coefficient is larger than 1.0, while that in our new method remains finite. This graph shows the overestimation problem is improved in our new method. The computation time for each friction coefficient was about 1120 CPU seconds on average for our new method.

B. Pushing Operation

Let us consider pushing operation of a cuboid on a plane (Fig. 7). The object reference frame is set as shown in the figure. The size of the object is $2 \times 2 \times 1$ and the mass of the object is 1 ($M_o = 1$). Then we have $\boldsymbol{Q}_{\text{known}} = (0, 0, -9.8, 0, 0, 0)^T$ and $\boldsymbol{R} = \text{diag}(1, 1, 1, 5/12, 5/12, 2/3)$. Friction coefficient is 0.3. All the robot fingers are in position-control mode.

Consider the case of Fig. 7 (a), where no robot fingers exist and the object is stationary. In this case, the robustness value is 2.94; that is, the object can resist disturbing force whose magnitude is up to 2.94 (in the sense of (23)). The value corresponds to the magnitude of the force required to slide this object horizontally ($1 \times 9.8 \times 0.3 = 2.94$). The computation time was 68 CPU seconds.

In the case of one-point pushing of the object at $(1, 0, 0)^T$ toward $(-1, 0, 0)^T$-direction (Fig. 7 (b)), the robustness value is zero; that is, this manipulation is not robust because an infinitesimal disturbance can perturb the motion of the object. The computation time was 36 CPU seconds in this case.

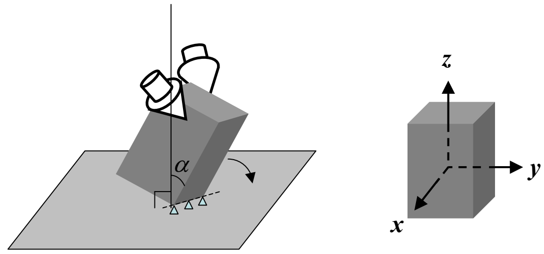

Fig. 8. Example: Tumbling a Cuboid

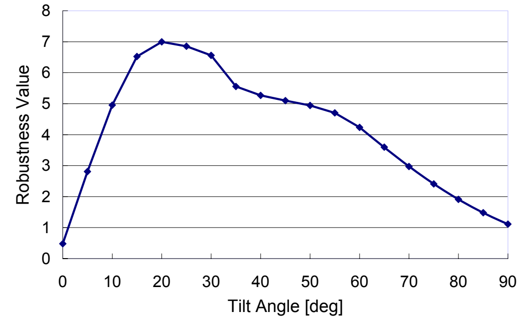

Fig. 9. Manipulation Robustness in Tumbling

On the other hand, in the case of two-point pushing at $(1, \pm 0.3, 0)^T$ (Fig. 7 (c)), the robustness value is 0.88; that is, the object can resist external disturbances whose magnitude is up to 0.88 (in the sense of (23)) without changing its motion. That corresponds to a "stable push" [3] by a position-controlled pusher with line contact. In this case, the computation time was 113 CPU seconds.

Those results show that our new method can deal with situations as shown in Fig. 2 appropriately.

C. Tumbling Operation

Let us consider tumbling a cuboid whose size is $1 \times 1 \times 2$ (Fig. 8). The object reference frame is set as shown in the figure. The mass of the object is 1 ($M_o = 1$). In this case, $\boldsymbol{R} = \mathrm{diag}(1,\, 1,\, 1,\, 5/12,\, 5/12,\, 1/6)$. The line contact between the edge of the object and the plane is approximated by three point contacts at $(\pm 1/2,\, 1/2,\, -1)$ and $(0,\, 1/2,\, -1)$.

Robot fingers pinch the cuboid at $(\pm 1/2,\, 0,\, 3/4)^T$; one finger is in position-control mode and the other is in force-control mode. The commanded normal force for the robot finger in force-control mode is 10 ($\boldsymbol{f}_{\mathrm{com}} = [0,\, 10]^T$). The relationship between the tilt angle (α) of the object and the robustness value is shown in Fig. 9. The robustness value is high around $\alpha = 20$ [deg]. The results match our intuition, because the center of mass of the object and the fingertip locations come directly above the contact edge at $\alpha = 16$ [deg] and at $\alpha = 27$ [deg], respectively. The computation time for each tilt angle was about 150 CPU seconds on average.

VI. Conclusion

In this paper, we proposed a new quantitative test of the robustness of quasi-static graspless manipulation. The test is composed of solving a series of linear programming problems. Numerical examples showed that the proposed method can evaluate the robustness of graspless manipulation more accurately than a previous study [10]. The improved accuracy results from the consideration of constraints on static frictional forces derived by Omata and Nagata [11] [12].

Developing more efficient calculation procedure should be addressed in future work. Reducing the computation time is very important for the application to planning of graspless manipulation [17] [18].

References

[1] Y. Aiyama, M. Inaba, and H. Inoue, "Pivoting: A new method of graspless manipulation of object by robot fingers," in *Proc. of IEEE/RSJ Int. Conf. on Intelligent Robots and Systems*, Yokohama, Japan, 1993, pp. 136–143.

[2] M. T. Mason, "Progress in nonprehensile manipulation," *Int. J. of Robotics Research*, vol. 18, no. 1, pp. 1129–1141, 1999.

[3] K. M. Lynch and M. T. Mason, "Stable pushing: Mechanics, controllability, and planning," *Int. J. of Robotics Research*, vol. 15, no. 6, pp. 533–556, 1996.

[4] K. B. Shimoga, "Robot grasp and synthesis algorithms: A survey," *Int. J. of Robotics Research*, vol. 15, no. 3, pp. 230–266, 1996.

[5] A. Bicchi and V. Kumar, "Robotic grasping and contact: A review," in *Proc. of IEEE Int. Conf. on Robotics and Automation*, San Francisco, CA, U.S.A., 2000, pp. 348–353.

[6] A. M. Okamura, N. Smaby, and M. R. Cutkosky, "An overview of dexterous manipulation," in *Proc. of IEEE Int. Conf. on Robotics and Automation*, San Francisco, CA, U.S.A., 2000, pp. 255–262.

[7] M. T. Mason and K. M. Lynch, "Dynamic manipulation," in *Proc. of IEEE/RSJ Int. Conf. on Intelligent Robots and Systems*, Yokohama, Japan, 1993, pp. 152–159.

[8] J. C. Trinkle, A. O. Farahat, and P. F. Stiller, "First-order stability cells of active multi-rigid-body systems," *IEEE Trans. on Robotics and Automation*, vol. 11, no. 4, pp. 545–557, 1995.

[9] H. Kijimoto, T. Arai, Y. Aiyama, and T. Yamamoto, "Performance analysis and planning of graspless manipulation," in *Proc. of IEEE Int. Symp. on Assembly and Task Planning*, Porto, Portugal, 1999, pp. 238–243.

[10] Y. Maeda and T. Arai, "A quantitative stability measure for graspless manipulation," in *Proc. of IEEE Int. Conf. on Robotics and Automation*, Washington D.C., U.S.A., 2002, pp. 2473–2478.

[11] T. Omata and K. Nagata, "Rigid body analysis of the indeterminate grasp force in power grasps," *IEEE Trans. on Robotics and Automation*, vol. 16, no. 1, pp. 46–54, 2000.

[12] T. Omata, "Rigid body analysis of power grasps: Bounds of the indeterminate grasp force," in *Proc. of IEEE Int. Conf. on Robotics and Automation*, Seoul, Korea, 2001, pp. 2203–2209.

[13] S. Hirai and H. Asada, "Kinematics and statics of manipulation using the theory of polyhedral convex cones," *Int. J. of Robotics Research*, vol. 12, no. 5, pp. 434–447, 1993.

[14] A. Bicchi, "On the problem of decomposing grasp and manipulation forces in multiple whole-limb manipulation," *Robotics and Autonomous Systems*, vol. 13, no. 2, pp. 127–147, 1994.

[15] X.-Y. Zhang, Y. Nakamura, and K. Yoshimoto, "Mechanical analysis of grasps with defective contacts using polyhedral convex set theory," *J. of Robotics Soc. of Japan*, vol. 14, no. 1, pp. 105–113, 1996, (in Japanese).

[16] M. H. Raibert and J. J. Craig, "Hybrid position/force control of manipulators," *ASME J. of Dynamic Systems, Measurement, and Control*, vol. 102, no. 2, pp. 126–133, 1981.

[17] Y. Maeda and T. Arai, "Planning of graspless manipulation by a multifingered robot hand," *Advanced Robotics*, vol. 19, no. 5, pp. 501–521, June 2005.

[18] K. Miyazawa, Y. Maeda, and T. Arai, "Planning of graspless manipulation based on rapidly-exploring random trees," in *Proc. of 6th IEEE Int. Symp. on Assembly and Task Planning*, Montreal, Canada, 2005, pp. ITP–3.